Chapter 5

H I absorption towards the Tycho's supernova remnant [1]

Introduction

The interstellar medium of a galaxy is the host of the star formation activities and plays a very crucial role in galactic evolution. It is not only the fact that in the interstellar medium (ISM) H I gas is indirectly involved in the star formation activities via conversion of H I into dense molecular H_2 gas, but it is now known that shielded gas of H I also proceeds to star formation even though the bulk of it is not converted to molecular phase (Krumholz, 2012; Zhou et al., 2018). Thus atomic hydrogen (H I) is understood to be the reservoir of the next generation's star formation. Furthermore, the energy injection from stellar feedback also break the H_2 into atomic and ionized gas. Hence studying the H I structures and its population in the different direction and locations in the Galaxy becomes essential to understand the Galactic evolution. At smaller scales (below pc), the detection of H I structures in the Galaxy is done using the H I absorption studies against bright background sources. At very small scales where pulsars are used as background sources, Frail et al.

[1] The work is to be submitted.

(1994) show that at scales of 5-100 au, opacity variation is observed along a few lines of sight in our Galaxy. A similar study in the other directions of Galaxy finds no evidence of optical depth variation (Johnston et al., 2003; Stanimirovi et al., 2003). Brogan et al. (2005) also demonstrated the opacity variation in the Galaxy at the scales of $\sim$ 10 au using the VLBI observations. The measurement of structure-function and power spectrum of optical depth along few lines of sight in the Galaxy show the existence of scale-invariant structures at au to parsec length scales (Deshpande et al., 2000; Dutta et al., 2014; Roy et al., 2010, 2012). The study of the small-scale structures in the Galaxy has been questioned whether to be a representative of any physical process or just transient entities, as they are observed along with few directions and not in other few directions in the Galaxy. The above question can be answered if we have enough observations of H I in the different directions in the Galaxy.

5.1 Tycho's Supernova remnant

From the recent observations, Tycho's remnants (also known as SNR1572 and 3C10) is found to belong to Type Ia supernova remnants (Krause et al., 2008). In the radio frequency observations, the center of the Tycho's SNR in the equatorial coordinate system is accepted to be at 00:25:18,+64:09:00 (J2000), and at 120.1,+1.4 in the Galactic coordinate system (Green, 2014). It belongs to the class of shell-type supernovae remnants having a maximum diameter of the shell $\sim$ 8' and shell width around 1' (Seward et al., 1983). The remnants of the Tycho's supernova is considered to be the candidate of the high energy electron acceleration (Katsuda et al., 2010). There is quite a debate in the literature about the distance of Tycho's SNR. The few measurements of the distance of Tycho's SNR are listed in table 5.1. This is also suggested to be located within the Perseus arm of the Galaxy (Lee et al., 2004).

Table 5.1 Various distance estimates of Tycho's SNR from diffrent refrences.

distance (kpc)	Methods/using	refrences
1.8-2.8	Expansion of filaments in SNR and shock velocity	Chevalier et al. (1980)
1.7-3.7	Observations of H I	Albinson et al. (1986)
2.0-2.8	Expansion of filaments in Tycho's SNR	Kirshner et al. (1987)
At 4.5	Observations of H I	Schwarz et al. (1995)
2.4-3.2	Fitting light curve of Tycho's SNR	Ruiz-Lapuente (2004)
2.3-4.7	Brightness distance relation	Krause et al. (2008)
3.0-5.0	Ejecta velocity and proper motions of Tycho's SNR	Hayato et al. (2010)
2.5-3.0	Observations of H I	Tian and Leahy (2011)
3.0-4.0	Comparison of Hydrodynamic simulation with IR data	Williams et al. (2013)
1.4-2.3	proper motions and distances of nearby stars	Ruiz-Lapuente et al. (2019)

Reynoso et al. (1999) studied the H I structures of ISM toward SNR Tycho at both small and large scales to explain the observed asymmetry in the direction of the Tycho's SNR. They suggested that the high-density of H I might be interacting with the SNR at the eastern side, accounting for the slow down in its expansion at the eastern edge. In the work, it was found that the properties of the local ISM might affect the dynamical evolution of supernovae remnants. Such studies were also performed by Lee et al. (2004), Cai et al. (2009) and Xu et al. (2011), where possible interaction between Tycho's SNR and the atomic or molecular cloud was reported at the northeast side of the SNR. These claims regarding the interaction of molecular cloud and Tycho's SNR at the eastern edge were rejected by Tian and Leahy (2011) using the absorption studies of ^{12}CO and H I in the line of sight of Tycho's SNR and a few other point sources in the surroundings of it. Recently Ruiz-Lapuente et al. (2019) re-examined the proper motions and distances of stars lying in the vicinity of Tycho's SNR, using the Second *Gaia* Data Release (DR2). They measured the kinematics and distances of the companions of the Tycho's SNR and showed that a particular companion star G (also referred to as Tycho G in their study) is the most favored star to be claimed as the companion of Tycho's SNR, at the distance of $1.95^{+0.60}_{-0.35}$ kpc, inferred from the parallaxes using the *Gaia* DR2. If we assume the star G to be the companion star of Tycho's SNR, then Tycho must be within the distance limit of star G. In the direction of Tycho's SNR, there are point sources around it which

produces the significant H I absorptions in their directions. Tian and Leahy (2011) did the absorption studies in the direction of the Tycho's SNR and point sources G120.56+1.21, G119.72+2.4, and G119.71+1.12. The absorption studies by Tian and Leahy (2011) in the direction of Tycho's SNR and point sources have shown that there exists windows of absorptions toward the point sources but not observed in the direction of Tycho's SNR. In the case of G120.56+1.21, there exist windows of absorptions toward this point source but not observed in the direction of Tycho's SNR even though the maximum angular separation between the southeast edge of the SNR and this point source is around 0.42 degree (transverse length scale $\sim$ 0.015 kpc); revealing the existence of multi-component atomic and molecular cloud in the direction of Tycho's SNR and its neighborhood. Here we extend the study of H I absorptions toward the Tycho's SNR and point source (known as source G120.56+1.21 in Tian and Leahy (2011)) at the southeast of Tycho's SNR with a fine velocity resolution ($\sim$ 0.32km/s) and statistical tools to find out whether the H I absorptions observed toward Tycho's SNR is really because of the multi-component cloud or due to an extended cloud. We also try to figure out whether Tycho's SNR lies within dense clouds of Perseus arm or in front of it.

5.2 Observation and Data Analysis

We observe the Tycho's supernova remnants using the L band of GMRT in observation cycle 34 under the project code `34_095`. Our observation runs on 19 September 2018 and 21 September 2018. At each of the observation day, about 5 hours and 10 minutes were spent on Tycho's SNR. The two-day observation was done to gather the data based on the requirement of the project, to measure the H I optical depth power spectrum in the direction of Tycho's SNR with a total of around 12-hour observation on it. Here we give results based on the data observed on the first day.

Table 5.2 Observation summary for GWB and GSB.

	GWB	GSB
Working antennas	28	28
Central frequency	1418.5 MHz	1418.5
Bandwidth	25 MHz	2MHz
Visibility integration time	10 sec	8 sec
Total observation time	7h30m	7h30m
Number of channels	6384	512
Channel resolution	1.526 KHz	4.0 KHz

We use here the same GWB data observed only on 19 September 2018 for absorption studies. This observation uses the wide band of GMRT (GWB), having a total of 16384 channels with a channel width of 1.526 kHz (in 1406-1431MHz), corresponding to a velocity resolution of 0.32 km/s. This gives us a temperature resolution of 4.2K. Details about the observations can be found in table 5.2. In table 5.3, we list the calibrators that were observed with Tycho's SNR. We choose the bandpass calibrators such that they have significantly less absorption from the Galactic H I (see Roy et al. (2013a)). The H I absorption towards Tycho's SNR is found to be well covered in the LSR velocity range -150 to 40 km/s (Tian and Leahy, 2011) which is about 0.9 MHz in our observation frame. We separate 2600 channels around the absorption features toward Tycho's SNR, which covers well the above LSR range and use it for further analysis. We perform the primary calibration using the calibrators. We also perform the calibration and flagging loop several times before we converge to expected statistics. The calibrated data was further re-examined for any undesired visibilities, both in target source and calibrators. Since Tycho continuum emission is rather strong and only one point source could be visible in the field of view, we do not attempt any self-calibration.

For calibration and image construction, we use Common Astronomy Software Applications (CASA) (McMullin et al., 2007). After calibration, we split our data set in the LSR range -136.88 to 71.95 km/s (frequency range 1420.165-1421.157 MHz), having 651 channels to proceed for multichannel imaging. We use the Hogbom (Högbom, 1974)

Table 5.3 Details of the calibrators for this observation.

Flux Calibrator	
Source	3C48
Flux density	16.50 Jy
Phase Calibrator	
Source	B2352+495
Flux density	2.36 Jy
Bandpass Calibrator 1	
Source	B1641+399
Flux density	8.00 Jy
Peak optical depth	0.0014
Bandpass Calibrator 2	
Source	J0120-153
Flux density	4.80 Jy
Peak optical depth	0.0067

version of the CLEAN algorithm to construct the multichannel and continuum image of the Tycho's SNR and point source at 00:29:45.475,+63.58.40.727 (J2000) (henceforth called point source). Multichannel imaging was done using the cube data spectral mode parameter along with the Briggs weighting scheme by setting the robust parameter equal to unity. We restrict ourselves to the baseline range of 1.3-40Kλ. This, on the one hand, reduces the RFI contributions from the GMRT central square and, on the other hand, reduces band ripple that may arise due to the presence of the strong extended source in the field of view. We made 0-5 Kλ multichannel and continuum images for visual reference. All the continuum images shown are made by averaging 300 channels that correspond to $\sim$ 0.45 MHz. We achieve the sensitivity of $\sim$ 4.5 mJy/beam per channel in the cube (resolution $\sim$ 0.32 km/s) of 1.3-40Kλ, for a beam of (Bmaj, Bmin) = (9.96",6.48"). To deconvolve the Tycho's SNR and point source together, a simultaneous CLEAN window was used for the point source along with Tycho's SNR.

5.3 Spectral Analysis and Result

We show the continuum image of Tycho's SNR in the figure 5.1(a), together with the point source (PS) marked with a circle. This image is made using the 0-25Kλ baseline range. Noise level in this image at off-source region is $\sim$ 2.5 mJy/beam for a Gaussian beam of (Bmaj,Bmin) = (22.54",12.66"). Figure 5.1(b) shows the zoomed version of the continuum images of the Tycho's SNR, made using the baseline range 0-5Kλ. The ring of the Tycho's SNR is clearly visible in this image. Based on the distance of the companion star G of the Tycho and angular width of the ring as mentioned in the earlier sections, the physical width of the ring is $\sim$ 0.6pc. For spectral analysis, we use a continuum image made using the baseline range 1.3-40Kλ. The noise level in this image at the off-source region is $\sim$ 2.2 mJy/beam for Gaussian beam (Bmaj, Bmin) = (9.96",6.48").

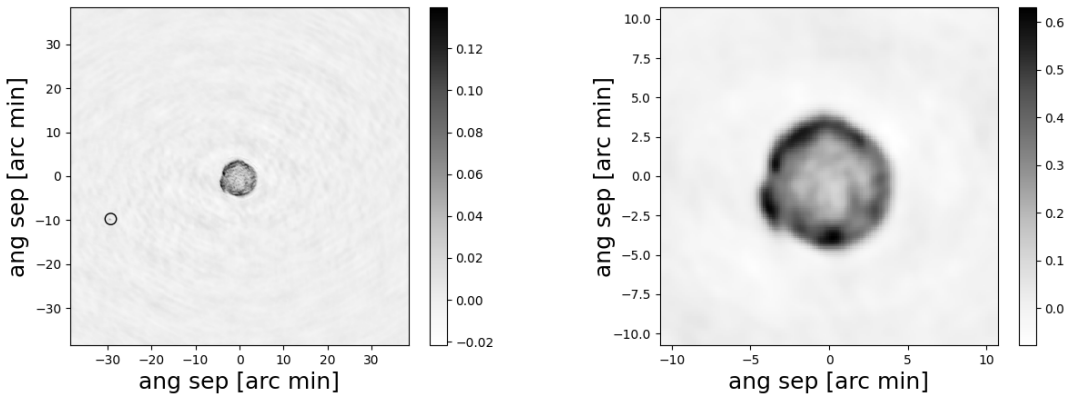

Fig. 5.1 : a) Countinumm image of the Tycho's SNR along with point source at 00:29:45.475, +63.58.40.727 (J2000) (inside circle) made using the baseline range 0-25Kλ. Since in our image only this point source is visible, so we will call it the point source at all refrences for it, b) Low resolution (0-5Kλ) countinumm image of Tycho's SNR. The numbers given in the horizontal and vertical axes in images correspond to pixels. For the 0-25Kλ image each pixel has a dimension of 4arcsec $\times$ 4arcsec. For 0-5Kλ, the pixel size is 8.0arcsec $\times$ 8.0arcsec.

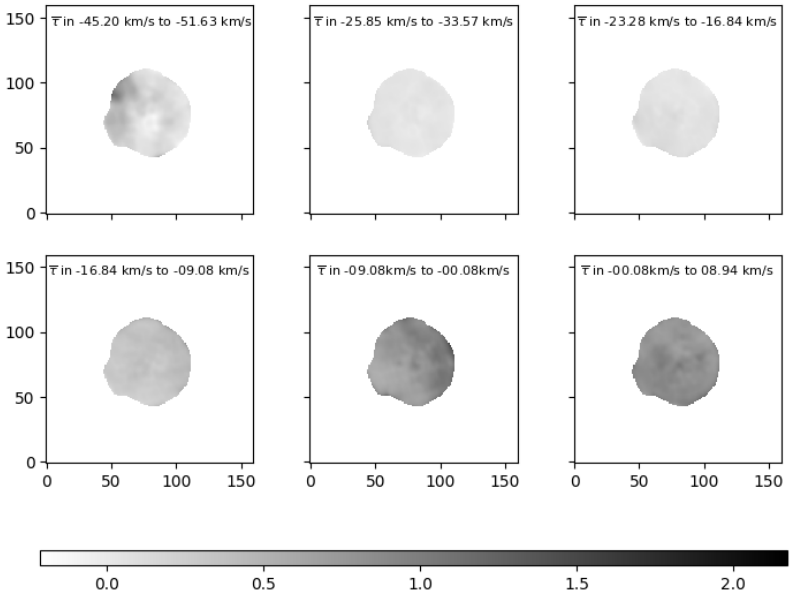

Fig. 5.2 : Figure shows the six optical depth images averaged in the velocity ranges, as shown in the labels. These images are made using the baseline range of 0-5Kλ. Optical depth images made by averaging in LSR velocity ranges from -25.85 km/s to -33.57 km/s, -23.28 km/s to -16.84 km/s, -16.84 km/s to -09.08 km/s,-09.08km/s to -00.08km/s and -00.08km/s to 08.94 km/s show significant absorptions at the overall face of Tycho's SNR, while in the range -45.20 km/s to -51.63 km/s, it shows higher absorption toward the eastern edge. The quantity shown in the image is optical depth and bar at the bottom of the image shows its magnitude.

We use the CLEAN algorithm on the calibrated visibility data to make the multichannel image (cube) of Tycho's SNR. Further, to obtain the optical depth image, we divide the cube by the continuum image. In figure 5.2, six optical depth images are shown, made using baseline range 0-5 Kλ and by averaging in the velocity ranges as shown in the figures. These images were made in the spectral windows of absorption toward Tycho's SNR. It is clearly visible from these images that in the LSR range of -09.08km/s to 08.94 km/s; which corresponds to the Local arm, the optical depth is relatively high and almost uniform over the face of Tycho's SNR. In the range of -45.20 km/s to -51.63 km/s, high optical depth is observed toward the eastern edge of Tycho's SNR, and it is almost absent in the other velocity ranges of -25.85 km/s to -33.57 km/s, -23.28 km/s to -16.84 km/s and -16.84 km/s to -09.08 km/s.

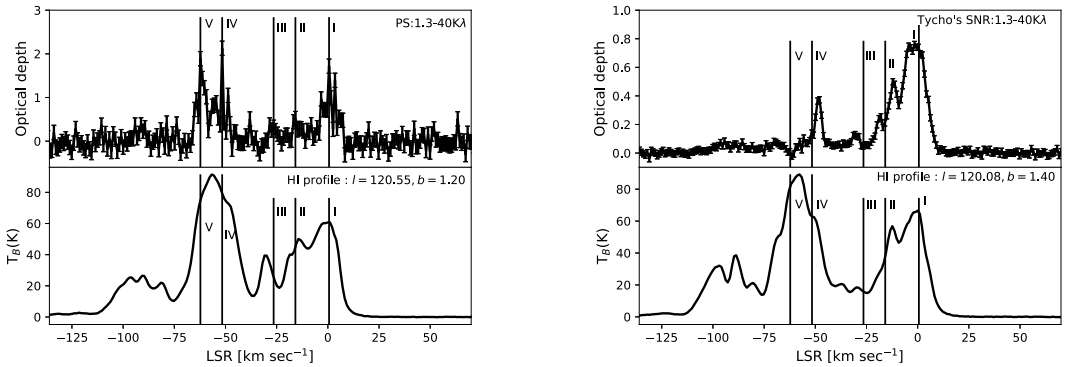

Fig. 5.3 : Optical depth spectra (with 1 σ error bars) of H I absorption towards point source (PS) and Tycho's SNR in the baseline range 1.3-40Kλ are shown as upper panels in the above figures. H I emission profiles, taken from LAB survey (Kalberla et al., 2005) in their directions with velocity resoluion of 1.30 km/s are shown as lower panels. The typical per channel sensitivity in brightness temperature for the LAB survey is $\sim$ 0.1 K. Vertical lines, marked as I, II, III, IV and V in these spectra show velocities 0.59 km/s, -15.84 km/s, -26.48 km/s, -51.62 km/s and -62.25 km/s and are made in refrence to the maximum absorptions in the direction of point source in the windows of its absorption as mentioned in the text.

To make the spectra of the overall face of the Tycho's SNR and to avoid the effect of any artifacts in it, we only use the pixels which are above 1σ noise and are inside the

circle of radius of 4.7' from its center. This avoids artifacts from the outside the SNR as well as from the inside the shell of the SNR. For the point source choosing the pixels above 1σ was not required as we have CLEANed it on a separate window of radius 0.5', which consists only of the point source. To make it free from the residual continuum, we fit the continuum part of the spectra using the second-order polynomial. Finally, optical depth spectra were generated using the spectra of the measured flux density. The Hanning smoothed optical depth spectra (with a resolution of $\sim$ 1 km/s) measured at the overall face of Tycho's SNR and in the direction of a point source using the baseline range 1.3-40Kλ are shown in the upper panel of figure 5.3. In the lower panels of these figures, we show the H I emission spectra in these directions as obtained from Kalberla et al. (2005)(LAB survey). Each channel in the optical depth spectra of the figure 5.3 corresponds to a temperature resolution of 38 K. Spectra toward Tycho's SNR show the absorption features in the velocity ranges of 10 to -23.73 km/s, -27.64 to -34.40 km/s and -45.0 to -52.77 km/s. Absorptions in the range 10 to -23.73 km/s correspond to the Local arm of our galaxy. The range, 10 to -23.73 km/s, also has many sub spectral features. The optical depth images shown in the figure 5.2, in the range -09.08km/s to 08.94 km/s belongs to the Local arm, while absorption in the ranges -45.20 km/s to -51.63 km/s belongs to the clouds between the Tycho's SNR and Local arm. The optical depth spectra toward the point source have spectral windows of absorptions as 10 to -6.30 km/s, -7.40 to -20.00 km/s, -23.00 to -31.63 km/s and -47.00 to -66.40 km/s, arising from the Local arm and other clouds in the line of sight. In figure 5.3 we have shown the velocity indices 0.59 km/s, -15.84 km/s, -26.48 km/s, -51.62 km/s, and -62.25 km/s by vertical lines and have marked them by I, II, III, IV, and V respectively to show the dissimilarities between the absorption seen in these directions of point source and Tycho's SNR.

In figure 5.4 we have compared the two optical depth spectra completely from two opposite regions of Tycho's SNR along with spectra seen toward the point source. Four optical

depth spectra of 4 consecutive regions of Tycho's SNR from the eastern part are shown in the right panel of figure 5.4. In these figures, we have also shown the marked velocities I, II, III, IV and V. From the figure 5.4 it is also clear that in the direction of the point source, there is absorption at larger -ve velocities but not in the direction of Tycho's SNR and optical depth spectra seen in the left side of Tycho's SNR is different from those of right side indicating the possibility of different H I cloud structures at the face of Tycho's SNR. The difference between the spectra from the left (eastern) and right (western) side of Tycho's SNR and similarity between spectra from the left (eastern) region of Tycho's SNR with point source motivates us to perform the statistical procedure of correlation i.e., Similarity index and Spearman's rank correlation between the spectra of the point source and regions of Tycho's SNR. We perform these correlation methods to see any correlation between spectra, statistically.

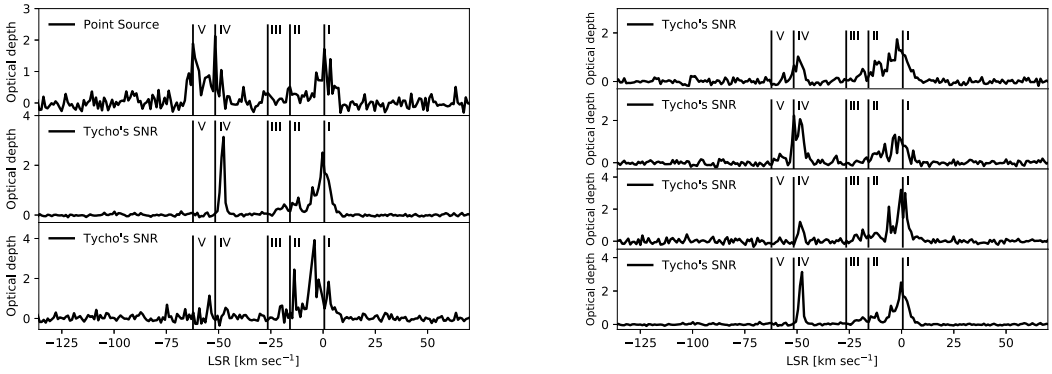

Fig. 5.4 : Left: Comparisons of the optical depth spectra of point source with two optical depth spectra toward the left and right face of Tycho's SNR. Right: Four spectra of optical depth toward the left region of Tycho's SNR. The velocity resolution of the spectra is 1km/s. The marked vertical lines refers to the velocities as shown in figure 5.3.

In the view of the optical depth image in velocity range -45.20 km/s to -51.63 km/s (shown in figure 5.2) and to measure, if there is multi-component of H I cloud toward the Tycho's SNR, we divide the Tycho's SNR in 21 regions where each region is taken as a circle of radius 44" (see figure 5.5). These regions are made at the circles of the outer and

inner radii of 228" and 98" respectively (using the center 00:25:19.8,+64.08.10 (J2000)). All regions and spectra associated with them can be seen in figure 5.5. From figure 5.5 we see that in the eastern part of the Tycho's SNR, the velocity component IV, which has significant absorption, is present while it is absent in the spectra from the western part of the Tycho's SNR.

Similarity index: Considering two spectra $\tau_1(v)$ and $\tau_2(v)$ measured at discrete frequency channels, we quantify their similarity using the similarity index $S_n(v)$. We first calculate $\Gamma_{1,2}(v)$ by convolving both spectra by a tophat window function. We estimate the absolute difference between the spectra $d(v) = |\Gamma_1(v) - \Gamma_2(v)|$ and normalize it by the maximum of $\Gamma_{1,2}(v)$, i.e, Γ_{max}, to get $D(v) = \frac{d(v)}{\Gamma_{max}}$. The similarity index of order n is defined as

$$S_n(v) = \exp^{[-D(v)^n]}. \tag{5.1}$$

Note that, if the two spectra are exactly the same, the argument of the exponent is zero and we get a similarity index of unity. If they differ much, then the similarity index approaches zero. The normalization by Γ_{max} ensures that we only consider the relative differences.

Spearman's rank correlation and p value: To measure the strength of correlation between the two data sets, which are of monotonic type, we use Spearman's rank correlation. Let us assume $\tau_1(v)$ and $\tau_2(v)$ represents the two diffrent spectra measured at n discrete frequency channels. We choose a top hat window centered at a frequency v and width δv and consider the spectral measurements within this window. The rank values of these spectral measurements $u(v)$ and $v(v)$ for $\tau_1(v)$ and $\tau_2(v)$ respectively are defined as the position of a particular τ value in the assending order. Difference between these rank values is $d(v)$. The spearman correlation calculated at v is defined as

$$r(v) = 1 - \frac{6\sum d(v)^2}{n(n^2-1)}. \tag{5.2}$$

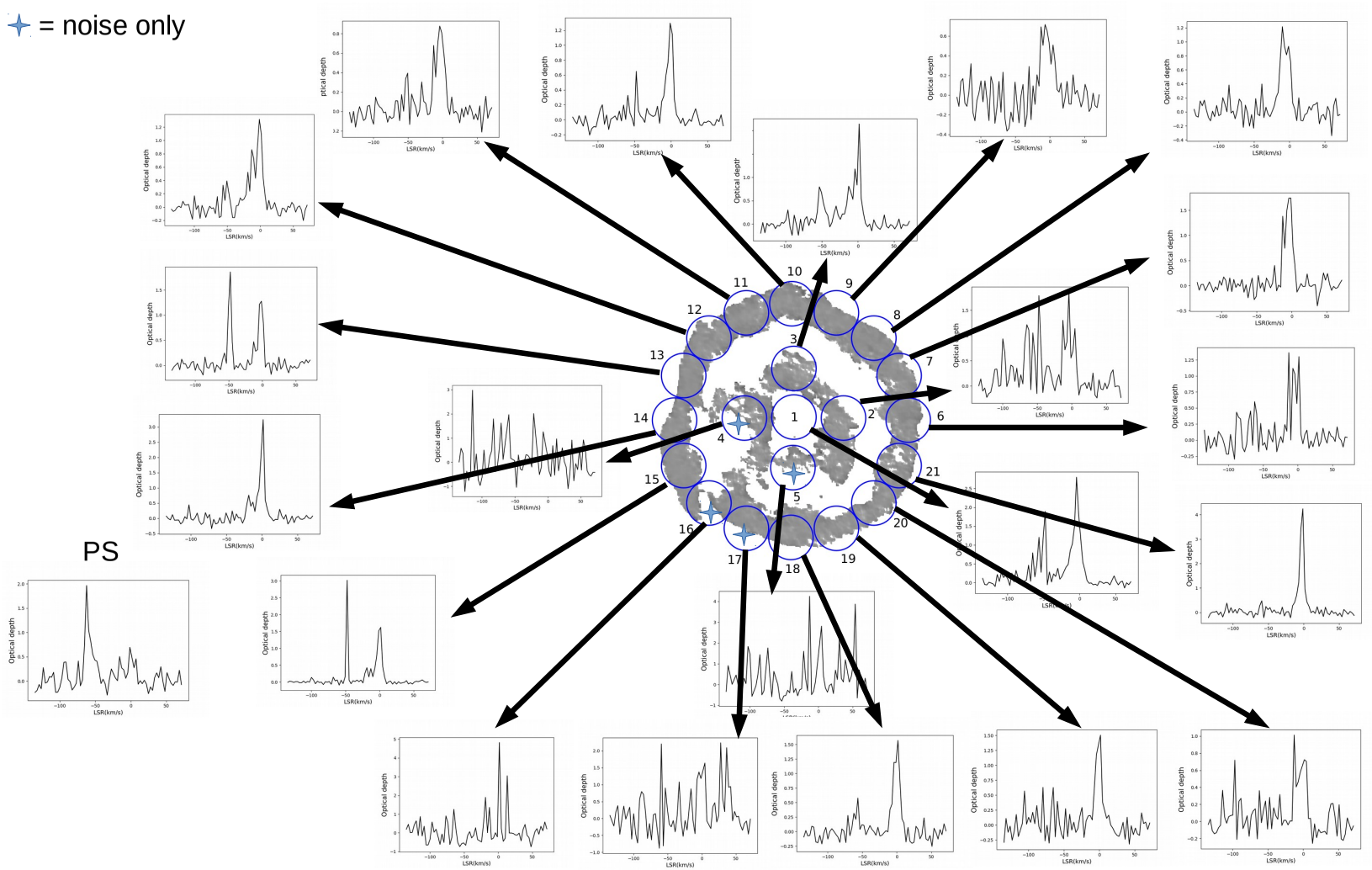

Fig. 5.5 : Optical depth spectra for different regions along with spectra of point sourec (PS) are shown. The figure helps to easily compare the spectra correlated with each other.

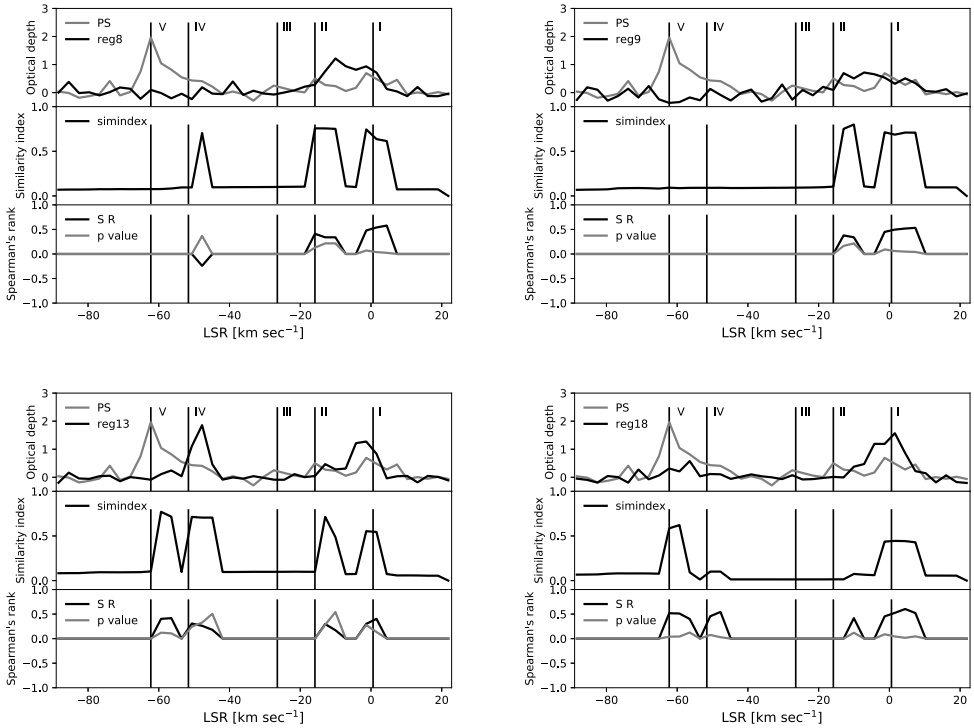

Fig. 5.6 : Similarity index and Spearman's rank (S R) correlation between the spectra of the point source (reg 0) and four diffrent regions (reg8, reg 9, reg13 and reg18) of Tycho's SNR. Vertical lines represents the marked velocities as shown in figure 5.3

In case of strong correlation, no correlation and anticorrelation, $r(\nu)$ have values of +1, 0, -1 respectively. In the figures 5.6 we have shown Spearman's rank correlation along the y axis in the lower panel of each subfigure. We also have shown the p-value in the same lower panel which gives the chance correlation. From these analyses, we see that both the similarity index and Spearman's rank correlation are different for different regions. The correlation between absorption component IV from the eastern regions the Tycho's SNR and absorption component V of point source seems not to be by chance. It may be the result of an extended cloud from the face of Tycho's SNR toward the point source. The other two absorption components, I and II of the point source and regions of Tycho's SNR, are also found to be correlated, but absorption components III and V do not show any correlation.

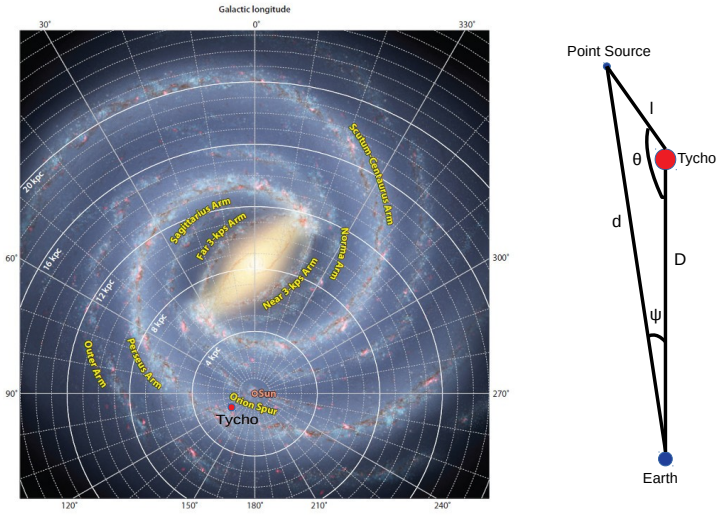

Fig. 5.7 : Approximate location of Tycho's SNR (red dot) in our Galaxy and geometry to calculate the excess velocity of cloud in the direction of the point source. The left figure is taken from Annu.Rev.Astron.Astrophys(2012), originally made by R. Hurt (in collaboration with R. Benjamin) and available in Churchwell et al. (2009). The figure of galactic structures (in the background) first appeared in Astronomical Society of the Pacific (Copyright 2009,Astron.Soc.Pac.)

5.4 Discussion and Conclusion

The absorption toward Tycho's SNR by the Local arm shows absorption in the wide velocity width i.e. from -23.73 km/s to 10 km/s, which is much larger than the absorption window of -45.0 to -52.77 km/s. This is opposite to the absorption windows seen toward supernova remnants Cassiopeia-A (Roy et al., 2010) where absorption window from Local arm is much narrow in comparison to the absorption window due to Perseus arm showing the quite different H I structures in front of these supernova remnants in these two directions even though they are nearby supernova remnants on Galactic length scales. The narrower absorption features toward Tycho's SNR, which is expected to be because of Perseus arm, might be because of the fact that Tycho's SNR is either just inside the Perseus arm or there is no enough H I cloud density at this site to produce the absorption over the larger velocity window. The absorption from the Local arm is present at all over the face of Tycho's SNR and point source, but absorption due to the Perseus arm is mostly not present toward the western side of Tycho's SNR, showing the H I distribution irregularity at this site. This also indicates another possibility that Tycho's SNR is not deep inside any arm rather than being just behind the local arm, and there may exist the cloud that produces the absorption in the LSR velocity range of -45.0 to -52.77 km/s. Our correlation analysis between the optical depth spectra of the point source at $\sim$ -61 km/s (V component) and those from western regions of the Tycho's at $\sim$ -48.5km/s (IV component) shows that there might be cloud extending from the face of Tycho's SNR to towards point source. We believe that an extended cloud model would be a proper explanation (see figure 5.7) for this correlation.

Tian and Leahy (2011) suggested that absorption at $\sim$ -61 km/s in the direction of the point source is the result of the cloud existing behind the Tycho's SNR. They also estimated the distance of the this SNR to be somewhere bwteen 2.5-3.0 kpc based on the observations of the HI. The distance estimation of the Tycho's SNR based on the brightness distance rela-

tion gives a distance of the 2.3-4.7 kpc (Krause et al., 2008). In a recent work, comparison of the Hydrodynamic simulation with IR data shows gives distance estimates of Tycho's SNR as 3.0-4.0 kpc (Williams et al., 2013). Considering Tycho G star is the companion of Tycho's SNR, the distance is expected to be $1.95^{+0.60}_{-0.35}$ kpc (Ruiz-Lapuente et al., 2019). We assume that Tycho SNR is at the near end of the Perseus arm, then the cloud near to Tycho's SNR must show absorption at $\sim$ -25 km/s, as it comes from distance and LSR velocity conversion method suggested by Wenger et al. (2018), which uses the Galactic rotation method with the updated solar parameters for the distance conversion. But the maximum absorption toward Tycho's SNR is at $\sim$ -48.5 km/s suggesting that near the end of the cloud (at the face of Tycho's SNR) must have an excess velocity of $\sim$ -23.5 km/s. If the same excess velocity is also assumed to be at the far end of the cloud, then it must have velocity $\sim$ -36.8 km/s due to galactic rotation suggesting it to be existing at the distance of $2.89^{+0.69}_{-0.63}$ kpc behind the Tycho's SNR. Reynoso et al. (1999) have suggested the presence of an extended H I structure at the eastern edge of the Tycho's SNR. From the outcomes of our results, we suggest that the size of the extended cloud be $\geq$ 1kpc. In figure 5.7 we have shown the possible geometry (as a reference) showing Tycho's SNR, an elongated cloud, and earth in Galactic frame to find the length and orientation of the possible extended cloud. From the geometry of the cloud shown in the figure, it is simple to figure out that,

$$l^2 = d^2 + D^2 - 2d \times Dcos(\psi) \tag{5.3}$$

and

$$d^2 = l^2 + D^2 - 2l \times Dcos(\theta) \tag{5.4}$$

Hence we can determine θ since other values ψ, d and D are known. Using the geometry as shown in figure 5.7 and equations 5.3 and 5.4 we found $\theta \sim 180$ degree as expected if near end of cloud (at face of Tycho's SNR) and far end of cloud exist at the distance of 1.95 and 2.89 kpc respectively.

In this chapter, we studied the spectral features of the H I absorptions in the line of sight of the Galactic, Tycho's supernova remnants, and an unresolved source in the neighborhood line of sight of this SNR. From the optical depth spectra measured across the face of Tycho's SNR, we find the non-symmetric distribution of the H I structures across its face. The spectral component IV is not present at the western side of the SNR. The spectral component V, which is present in the direction of the point source, is not present in the direction of the SNR. We carry out the correlation analysis between spectral component V in the direction of point source and spectral component IV in the direction of the SNR. We find that these two components are correlated, suggesting the existence of extended structures at the eastern edge of Tycho's SNR.

Based on the distance of the most favored companion of the Tycho's SNR, we calculated the excess velocity of the H I cloud in the direction of these two sources. The excess velocity of the CNM clouds in the direction of these two sources is found to be $\sim$ -23 km/s. Using the distance velocity relation for the galactic objects, we calculated the distance of the cloud producing the maximum absorption in the direction of the point source and concluded that the H I structures between these sources must extend beyond 1kpc. Based on the observed spectral features in the direction of the Tycho's SNR, we propose that the site of the Tycho's SNR not be in deep H I clouds, but it should be at the edge of the Perseus arm behind the Galactic Local arm.